doi:10.3969/j.issn.2095-0411.2019.05.006

Size Distribution in Self Assembled Solid State Si Quantum Dots

JIA Xuguang[1], ZHANG Tian[2], LIN Ziyun[2], CONIBEER Gavin[2]

(1. School of Materials Science & Engineering, Changzhou University, Changzhou 213164, China; 2. School of Photovoltaic and Renewable Energy Engineering, University of New South Wales, Sydney, New South Wales 2052, Australia)

Abstract: In the previous work, a model was proposed to quantitatively explain the PL spectrum of colloidal Si quantum dot (QD) by inducing the quantum confinement effect and particle size distribution. In this work, this method is adapted for size distribution analysis of QDs in a solid matrix. Results shows that the size distribution of QDs in these solid samples is more widely spread compared to colloidal one. The possible reason is the lack of constraint in horizontal directions in these samples and thus the QDs become ellipsoidal. The wide distribution of QD size will cause the spread of bandgap and reduce the quantum confinement effect which limits the practical application of such materials.

Key words: silicon quantum dots; size distribution; photovoltaics; photoluminescence

自组装固体硅量子点中的粒径分布

贾旭光[1], ZHANG Tian[2], LIN Ziyun[2], CONIBEER Gavin[2]

(1. 常州大学 材料科学与工程学院,江苏 常州 213164;2. 新南威尔士大学 光伏与可再生能源学院,澳大利亚 悉尼 2052)

摘要:提出了一个用来定量分析胶体硅量子点光致荧光光谱的模型,得到量子点的粒径分布,并将此方法应用于固体硅量子点材料粒径分布的分析。结果表明:与胶体硅量子点相比,固体样品中硅量子点粒径分布更宽。这可能是由于固体样品硅在结晶过程中水平方向缺乏约束,因此形成的量子点为椭球形。纳米硅中粒径分布太宽会导致材料带隙分布变宽。减少量子约束效应,限制了这些材料在实际中的应用。

关键词:硅量子点;粒径分布;光伏;光致荧光

中图分类号:TK 8 **文献标志码**:A **文章编号**:2095-0411(2019)05-0036-06

收稿日期:2019-03-14。

作者简介:贾旭光(1988—),男,山西朔州人,博士,讲师。E-mail: x.jia@cczu.edu.cn

引用本文:JIA X G, ZHANG T, LIN Z Y, et al. Size Distribution in Self Assembled Solid State Si Quantum Dots [J]. Journal of Changzhou University(Natural Science Edition), 2019, 31(5): 36-41.

Si nanocrystals (Si NCs) or interchangeably quantum dots (QDs) embedded in an oxide matrix are promising materials for all-Si nanostructure tandem solar cells or selective contacts for hot carrier solar cells [1-4]. To realize such efficient photonic devices, a tight control over size and a narrow size distribution are necessary. Zacharias et al proposed an effective method to preparing superlattice structure with Si QD[5]. Alternating thin layers of a SiO_2 followed by a silicon-rich oxide (SRO) are deposited onto a suitable substrate. This structure may be referred to as "SRO/SiO_2 multilayers"[6]. The thickness of each thin layer is in order of a few nanometers. The samples are then annealed at 1100 ℃ in N_2 atmosphere for 1 hour. The size of such QDs are expected to correspond with the thickness of SRO layer as their growth is constrained by the SRO layer. Such Si QDs have been fabricated by co-sputtering deposition of silicon rich layers interspersed with stoichiometric SiO_2 layers[2,6]. Even for this synthesis method, the size distribution of QDs cannot be avoided and should be studied. However, the size distribution of Si QDs embedded in a matrix is very difficult to obtain, considering their non-uniform shapes and remarkable difficulties in TEM imaging [5,7-9]. In the previous work, we propose a model to quantitatively explain the PL spectrum of colloidal Si QDs by inducing the quantum confinement effect and particle size distribution. The size distribution information of Si QDs can be extracted from PL fitting naturally[10]. This model provides a reliable and non-destructive method and thus in this work we apply it to analyse the size distribution of QDs in a solid matrix.

1　Experimental Details

To investigate the effect of silicon quantum dots size distribution, 3 samples with various multilayer structures are fabricated. Alternating SiO_2 and Si rich oxide (SRO) layers were deposited on quartz substrate using an AJA ATC-2200 sputtering system with RF power sources. The Si volume ratio in SRO layer was controlled at 70% by adjusting the RF power applied to the Si and SiO_2 targets. Ar flow rate and chamber pressure during the sputtering process were maintained at 15 sccm and 1.5 m Torr respectively. Sample A and Sample B are monolayer structure which consist 1 SRO/SiO_2 bilayer with thickness of SRO layer 3 nm and 4 nm respectively. Sample C is multilayer structure which consists 30 SRO/SiO_2 bilayers with thickness of SRO layer 4 nm. The thickness of SiO_2 layer of all these samples is 2 nm. The data of reference colloidal Si QD sample are from our previous report.[11] PL measurements were performed at room temperature using a semiconductor laser with 405 nm wavelength through an OD 3.5 attenuator and the full power of the laser was 25 mW before attenuation. The semiconductor is still non-degenerated under such illumination[11].

2　Results and Discussion

Figure 1 shows the PL spectra of these samples. It can be seen that the peak position of PL has an obvious blue shift as the dot sizes decreases. Such tunability of emission peak can be explained by the quantum confinement effect. Compared with bulk material, the breadth of the PL peak increases which can be explained by the size distribution of the dots. The size distribution causes a distribution of bandgap that broadens the PL spectrum[11].

Under the illumination condition in this experiment, the PL emission is dominated by spontaneous emission. As a result, we only need consider the spontaneous emission R_{sp} in this PL model as below

$$R_{sp}(\hbar\omega)=D(\hbar\omega)\sum_{a,b}B_{a\to b}N_a N'_b\delta(E_a-E_b-\hbar\omega)$$
$$=D(\hbar\omega)\iint B_{a\to b}n_a n'_b\delta(E_a-E_b-\hbar\omega)\mathrm{d}E_a\,\mathrm{d}E_b \quad (1)$$

Where $D(\hbar\omega)=\frac{n^3(\hbar\omega)^2}{\pi^2\hbar^3c_0^3}$ is the number of states per unit energy range, n is the refractive index, c_0 is the velocity of light in vacuum. N_a, N'_b are the electron and hole occupation number at energy level a and b respectively, $n_a n'_b$ is the density of states of the electron-hole pairs. $B_{a\to b}=\frac{4\pi^2e^2}{m^2n^2\omega}|\langle a|\hat{p}|b\rangle|^2$, is linked to the optical transition matrix element $|\langle a|\hat{p}|b\rangle|^2$

Under non-degenerationcondition, the PL intensity energy $I(\omega)$ can be expressed as:

$$I(\hbar\omega)\propto\int_0^{\hbar\omega}(\hbar\omega-E_g)^2(\hbar\omega)^2e^{-\frac{\hbar\omega}{kT}}e^{\frac{\Delta F}{kT}}\cdot f(E_g)\mathrm{d}E_g \quad (2)$$

Where k is the Boltzmann constant, E_g is bandgap, $\hbar\omega$ is the emitted photon energy. $\Delta F=E_{Fn}-E_{Fp}$ and E_{Fn} is the electron quasi Fermi energy and E_{Fp} is the hole quasi Fermi energy, $f(E_g)$ is the probability density function (PDF) of the bandgap. Since we adopted a log-normal size distribution for nanoparticles, the bandgap distribution function can be obtained as explained below[11-13]

$$f_{EG}(E_g)=\frac{1}{\sigma\left(\frac{C_1}{E_g-E_{g\_bulk}}\right)^{\frac{1}{2}}\sqrt{2\pi}}\exp\left(-\frac{\left(\ln\left(\left(\frac{C_1}{E_g-E_{g\_bulk}}\right)^{\frac{1}{2}}\right)-\ln(d_0)\right)^2}{2\sigma^2}\right)\cdot\frac{1}{2}\cdot C_1^{\frac{1}{2}}\cdot(E_g-E_{g\_bulk})^{-\frac{3}{2}} \quad (3)$$

Where d_0 is the geometric mean and σ is the geometric standard deviation of the QD diameter. E_{g_bulk} is the bandgap of the bulk material, d is the diameter of nanocrystals and C_1 is a coefficient lumping all other parameters for the quantum confinement effect and use 2 eV · nm^2 here [1,14-15].

Using Eq.1 and Eq.2, we can fit the PL spectrum by adjusting d_0 and σ. The detailed fitting parameters are shown in Table 1. The best fits are shown in Figure 1. From the PL spectra fitting, the QD size distribution histogram of these sample can be extracted by log-normal distribution function

$$f_D(d)=\frac{1}{\sigma d\sqrt{2\pi}}\exp\left(-\frac{(\ln d-\ln d_0)^2}{2\sigma^2}\right) \quad (4)$$

Table 1 Size distribution of Si QD Samples

Samples	Structure	O/Si ratio in SRO layer	d_0/nm	σ	Down boundary of 95% confidence interval/nm	Up boundary of 95% confidence interval/nm
A	3 nm, 1 layer	0.7	3.20	0.37	1.74	5.87
B	4 nm, 1 layer	0.7	3.95	0.45	1.89	8.26
C	4 nm, 30 bilayers	0.7	4.10	0.54	1.69	9.94
Reference sample	colloidal		3.70	0.20	2.66	5.11

These histograms are shown in Figure 2.

The size distribution for all samples is shown in Figure 2. It can be seen that the central position for each sample are 3.2 nm, 3.95 nm and 4.1 nm respectively, which correspond with the SRO thickness. Sample B and Sample C have the same SRO layer composition but different number of bilayers. The central position of these two samples are close to their SRO thickness. However, the spread becomes wider as the number of layer increases. For sample B, the size of 95% of the QDs is located between 1.74 nm to 5.87 nm, while for sample C, the size of 95% of the QDs is between 1.69 nm and 9.94 nm. This may be because in the multilayer system, the crystal easily penetrates the 2 nm barrier and from lager grain in the formation process. Mover, the distribution has an obvious skewness which means the QD size is not evenly distributed and spread more in the large size side. Due to the relation between the bandgap and QD size, the quantum confinement effect will be reduced for the larger crystals. This can be seen in the normalized bandgap distribution in Figure 4.

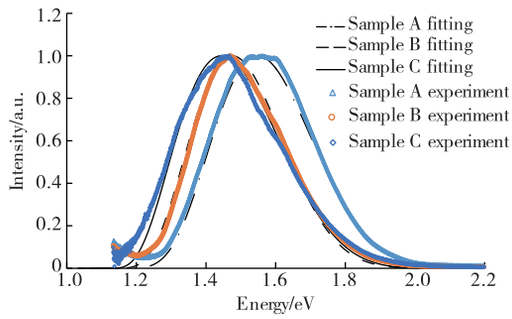

Fig.1　Experimental PL data and fitting

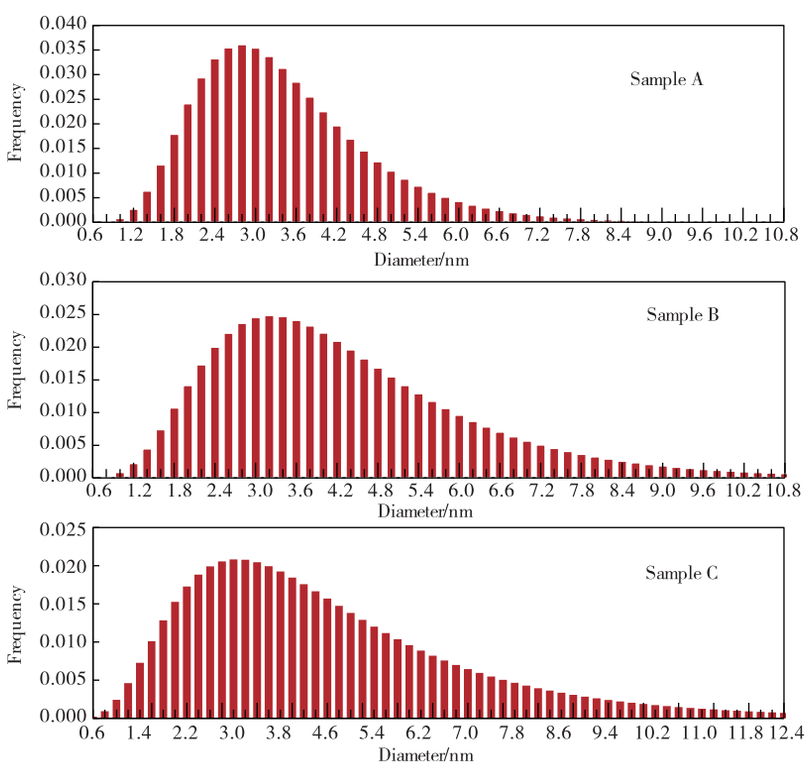

Fig.2　Histograms of the Si QD size from PL fitting

In addition, it can be seen that all these solid state Si QD samples have a wider size distribution compared with colloidal sample, which has negative effects on their practical application. This may be because in thicker SRO layer, the silicon nanocrystal has more space to grow in the horizontal direction and the QD becomes ellipsoidal. This can be seen from the high resolution TEM image of the

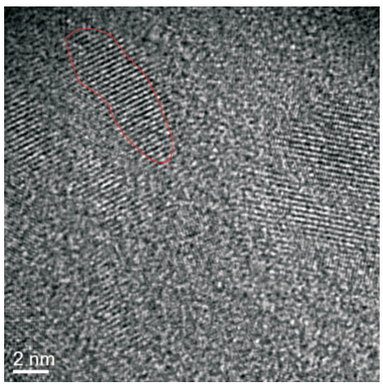

Fig.3 High resolution TEM of annealed Si QDs

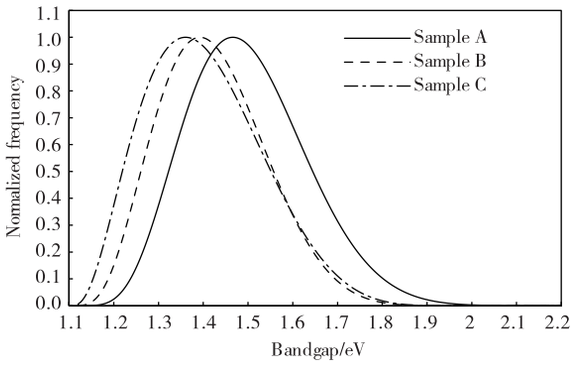

Fig.4 Simulated normalized bandgap distribution

annealed Si QD sample (V(O) : V(Si) ratio is 0.7) with 30 bilayers on Si substrate as shown on Figure 3. Kourkoutis et all has reported that Si concentration in the SRO layer has influence on the size and shape of the QD[7]. For a high Si concentration sample, the QD size will correspond with the SRO layer thickness but its shape become ellipsoidal and has a wide size distribution. For a low Si concentration sample, the shape of QD is more spherical but the size is smaller than the SRO thickness. The Si concentration of the sample used in this work is relatively high and we can see that their sizes generally correspond with SRO thickness but have wide distribution. This is consistent with Kourkoutis's report. It will be a considerable issue for the practical application because such large bandgap distribution will induce undesirable band states and cause inhomogeneity of the material. However, the conductivity will be a problem if we reduce the Si concentration. Therefore, the optimal Si concentration is the key factor to realize uniform QDs with considerable conductivity and should be further investigated in such solid state Si QD samples.

3 Conclusion

Now we have the capability to quantitatively analyse the size distribution of sputter annealed Si QD samples from the PL spectra. We have seen that the size distribution is more widely spread compared to colloidal as reference. This may be mostly because of the distribution in horizontal direction and become prominent in higher silicon content samples. As well as this, with the number of layer increasing the spread becomes wider. This may be due to the penetration of nanocrystals in barrier layers. The wide distribution of QD size will cause the spread of bandgap and reduce the quantum confinement effect which limits the practical application of such materials.

References:

[1]CONIBEER G, GREEN M, CORKISH R, et al. Silicon nanostructures for third generation photovoltaic solar cells [J]. Thin Solid Films, 2006, 511/512: 654-662.

[2]CHO E C, GREEN M A, CONIBEER G, et al. Silicon quantum dots in a dielectric matrixfor all-silicon tandem solar cells[J]. Advances in OptoElectronics, 2007, 2007: 1-11.

[3]GREEN M A. Third generation photovoltaics: ultra-high conversion efficiency at low cost[J]. Progress in Photovoltaics: Research and Applications, 2001, 9(2): 123-135.

[4]JIA X G, PUTHEN-VEETTIL B, XIA H Z, et al. All-silicon tandem solar cells: Practical limits for energy conversion and possible routes for improvement[J]. Journal of Applied Physics, 2016, 119(23): 233102.

[5]ZACHARIAS M, HEITMANN J, SCHOLZ R, et al.Size-controlled highly luminescent silicon nanocrystals: A SiO/SiO_2 superlattice approach[J]. Applied Physics Letters, 2002, 80(4): 661-663.

[6]CHO E C, PARK S, HAO X J, et al. Silicon quantum dot/crystalline silicon solar cells[J]. Nanotechnology, 2008,19(24): 245201.

[7]KOURKOUTIS L F, HAO X J, HUANG S J, et al. Three-dimensional imaging for precise structural control of Si quantum dot networks for all-Si solar cells[J]. Nanoscale, 2013, 5(16): 7499-7504.

[8]TAN T T, SELVAN S T, ZHAO L, et al. Size control, shape evolution, and silica coating of near-infrared-emitting PbSe quantum dots[J]. Chemistry of Materials, 2007, 19(13): 3112-3117.

[9]BORCHERT H, SHEVCHENKO E V, ROBERT A, et al. Determination of nanocrystal sizes: a comparison of TEM, SAXS, and XRD studies of highly monodisperse $CoPt_3$ particles[J]. Langmuir: the ACS Journal of Surfaces and Colloids, 2005, 21(5): 1931-1936.

[10]JIA X, LIN Z, ZHANG T, et al. Accurate analysis of the size distribution and crystallinity of boron doped Si nanocrystals via Raman and PL spectra[J]. RSC Advances, 2017, 7(54): 34244-34250.

[11]JIA X G, ZHANG P F, LIN Z Y, et al. Accurate determination of the size distribution of Si nanocrystals from PL spectra[J]. RSC Advances, 2015, 5(68): 55119-55125.

[12]KISS L B, SÖDERLUND J, NIKLASSON G A, et al. New approach to the origin of lognormal size distributions of nanoparticles[J]. Nanotechnology, 1999, 10(1): 25-28.

[13]SÖDERLUND J, KISS L B, NIKLASSON G A, et al. Lognormal size distributions in particle growth processes without coagulation[J]. Physical Review Letters, 1998, 80(11): 2386.

[14]READ A J, NEEDS R J, NASH K J, et al. First-principles calculations of the electronic properties of silicon quantum wires[J]. Physical Review Letters, 1992, 69(8): 1232-1235.

[15]VAN BUUREN T, DINH L N, CHASE L L, et al. Changes in the electronic properties of Si nanocrystals as a function of particle size[J]. Physical Review Letters, 1998, 80(17): 3803-3806.

(责任编辑:李艳)